# Pulsed interleaved excitation fluctuation imaging
# Supporting Material

Jelle Hendrix,[†] Waldemar Schrimpf,[†] Matthias Höller,[†] and Don C. Lamb[†§]

[†]Physical Chemistry, Department of Chemistry, Munich Center for Integrated Protein Science (CiPSM) and Center for Nanoscience (CeNS), Ludwig-Maximilians-Universität München, Butenandtstr. 11, Gerhard-Ertl-Building, D-81377 Munich, Germany.

[§]Department of Physics, University of Illinois at Urbana-Champaign, 1110 W. Green St., Urbana, IL 61801.

# Supporting Materials and Methods

## Reagents

The aqueous buffer contained 50 mM $Na_2HPO_4$, pH 7.5 and 50 mM NaCl. For the 10-cP buffer, 46% (w/w) sucrose (BioXtra 99.5%, Sigma-Aldrich Chemie GmbH Munich, Germany) was added. This buffer had a calculated viscosity of 10.28 centiPoise (cP) at 20 °C. Buffers exhibited a negligible fluorescence background. The gene of Venus FP was subcloned between *Eco*RI and *Hind*III restriction sites in a pRSET-B plasmid, expressed in JM109(DE3) cells (Promega, Leiden, The Netherlands) and the protein was purified via affinity chromatography ($Ni^{2+}$ NTA, Qiagen, Venlo, The Netherlands) and stored in 50 mM Tris pH 7.5, 150 mM NaCl. Microscopy was performed in 8-well coverslips (#1 Nunc Lab-Tek Chambered Coverglass, Thermo Scientific, Braunschweig, Germany). Dyes employed in this work were ATTO488-COOH ($D$ = 370 µm²/s at 22 °C, ATTO-TEC GmbH, Siegen, Deutschland) and Rhodamine B ($D$ = 394 µm²/s at 22 °C, Sigma-Aldrich). For Venus FP, the coverslips were first incubated for 30 minutes with 1 mg/mL BSA (Sigma-Aldrich) to prevent non-specific absorption of the protein, and subsequently washed twice with the measurement buffer.

## Cell culture

HeLa cells (NIH Reagent program) were cultivated in low-glucose DMEM (Life Technologies, Darmstadt, Germany) supplemented with 10% heat-inactivated fetal bovine serum at 5 % $CO_2$ and 37 °C in a humidified atmosphere. For transfection, $2\times10^4$ cells per well were plated in the morning in 8-well coverslips. Transfections were performed in the evening with Extreme Gene 9 transfection reagent (Roche Applied Science, Mannheim, Germany) and plasmid DNA. The peGFP-C1 plasmid was obtained from Clontech (Saint-Germain-en-Laye, France) The pmVenus-C1 plasmid was constructed by replacing the eGFP gene with an mVenus gene in the original peGFP-C1 plasmid. The peGFP-mCherry and mVenus-mCherry plasmids were constructed by subcloning the mCherry gene between *Eco*RI/*Bam*HI sites of peGFP-C1. At 12-16h post-transfection, the cell medium was exchanged with phenol red-free OptiMEM (Life technologies) and measurements were performed at room temperature.

## PIE-FI microscope

A schematic of the PIE-FI microscope setup is shown in Fig. S1. The PIE-FI microscope was built around an Eclipse TE200 (Nikon) base. As an objective lens, a NA1.2 water immersion objective was used (Nikon CFI Plan Apo VC 60XWI). For green excitation, a pulsed Erbium-doped fiber laser with a fixed repetition rate of 27.4 MHz (FFS.SYS-CONT-COMP-TSHG, Toptica Photonics, Gräfelfing, Germany) was tuned to 561 nm to excite Rhodamine B or mCherry and served as the master clock for the laser driver module (Sepia II [PDL 828, SCM 828, SLM 828], Picoquant GmbH, Berlin, Germany) and the controller for the scanner. For blue excitation, a 475-nm pulsed diode laser (LDH-P-C-470) was used to excite ATTO488, eGFP or Venus. The blue laser was delayed ~18 ns electronically with respect to the green laser and was run just above the lasing threshold to ensure a narrow instrument response function. A low pass filter (KG5, Schott, Mainz, Germany) was used to remove any residual IR light from the 561 nm excitation beam. Laser powers were individually attenuated with continuous neutral density filter wheels (Thorlabs, Dachau/Munich, Germany), the laser beams were superimposed with a dichroic mirror (Chroma 500DCXR, AHF Analysentechnik) and coupled into the same single mode fiber (coupler: HRJC-23AF-400/700-P-20AC, fiber: QPMJ-A3A,3AF-488-3.5/125-3-5-1, OZ Optics, Ottawa, Canada). An achromatic broadband collimator (60FC-4-RGB11-47, Schäfter+Kirchhoff) ensured concentric and Gaussian beam profiles at the exit of the fiber. The excitation light was reflected towards the microscope with a polychroic mirror (Semrock Di01-R405/488/561/635, AHF Analysentechnik, Tübingen, Germany). The laser powers described in this work were measured after the polychroic mirror and are ~2.5× higher than in the sample. Fast X/Y beam scanning was achieved by placing two closely-spaced galvanometer scanners in the beam path (scanner: 6210H, controller: MicroMax 673 Series, Cambridge Technology, Planegg, Germany). The midpoint between the scanning mirrors was expanded and projected onto the back focal plane of the objective through an achromatic Keplerian telescope (achromatic lens doublets AC254-050-A and AC254-200-A, Thorlabs), slightly overfilling the back aperture. Emission light was descanned, transmitted through the polychroic mirror and focused on an 80-µm pinhole by a 100-mm achromatic lens (AC254-100-A, Thorlabs). After the pinhole, the fluorescence was recollimated, spectrally split (565DCXR, AHF), spectrally filtered and focused on avalanche photodiodes (SPCM-AQR-12 and SPCM-AQR-14, Perkin-Elmer). Each APD was connected to a separate TCSPC card (SPC-140, Becker&Hickl), eliminating the need for a routing bit in

the photon files and reducing dead-time effects. Furthermore, TCSPC cards were hardware triggered over a data acquisition device (USB-6008, National Instruments) to ensure synchronization. A Chroma ET520/40 (AHF) emission filter was used in the green channel while a Chroma ET630/75 (AHF) emission filter was used in the orange/red channel (Fig. S2). To efficiently suppress the detection of scattered laser light, these emission filters were chosen that blocked both lasers at least OD6. For the lifetime filtered RICS experiments, a Semrock Brightline 525/45 (AHF) was used in the green channel. The microscope was aligned by optimizing the PSF radii with point FCS measurements and the homogeneity of the scanning field was checked by evaluating the PSF at different positions in the image (Fig. S3). The scanner was controlled by an arbitrary waveform generating PCI board (M2i.6034, Spectrum Systementwicklung Microelectronic GmbH, Grosshansdorf, Germany). The data acquisition software for the dual-color PIE-FI setup that controls the TCSPC and PCI cards, was written in the C# language in Microsoft Visual Studio 2010. The software generated an ASCII info file as well as photon files for each TCSPC card per image frame, avoiding the generation of large files.

## Image processing for correct RICS and N&B analysis

### *Removal of frames containing undesired heterogeneities*

During RICS measurements, impurities or heterogeneities such as protein aggregates or vesicles occasionally diffuse through the region of interest. As the RICS correlation functions are determined on individual frames, frames with undesired heterogeneities can simply be deleted from the movie before the analysis is performed. To check for frames containing fluorescent heterogeneities, thresholding was performed. First of all, a spatial average was calculated for all frames:

$$\langle I(x,y,f)\rangle_{\Delta(XY)} = \frac{1}{(2\Delta X+1)(2\Delta Y+1)} \sum_{x=-\Delta X}^{\Delta X} \sum_{y=-\Delta X}^{\Delta X} I(x,y,f) \qquad \text{Eq. S1}$$

where $\Delta X$ and $\Delta Y$ define the size of the averaging area. When the averaged pixel count in a spatially averaged region $\langle I(x,y,f)\rangle_{\Delta(XY)}$ was above a chosen threshold value, the frame was removed from the image series. For example, an averaging area $\Delta X$, $\Delta Y = 2$ and a threshold

of 5 could be used to efficiently remove impure frames from a Venus FP sample with a 50-kHz average image intensity.

***Image pre-processing for RICS***

With RICS, the spatial fluctuation of photon counts in images is quantitatively analyzed. For experiments in live cells, slow motions of the cell itself or organelles within the cell can mask the motion one wishes to detect. Even immobilized particles will contribute to the RICS correlation functions. For an ideal RICS analysis, the spatial fluctuations should be only due to diffusion of the molecules of interest. To correct for immobile heterogeneities, an *immobile mean correction* was applied to the images (1):

$$I_{\mathrm{RICS}}(x,y,f) = I(x,y,f) - \langle I(x,y)\rangle_F + \langle I\rangle_{XYF}, \qquad \text{Eq. S2}$$

where $I(x,y,f)$ is the photon count of pixel $(x,y)$ in frame $f$, $\langle I(x,y)\rangle_F = \frac{1}{F}\sum_{f=1}^{F} I(x,y,f)$ is the 'mean image' with the mean pixel intensities over all frames $F$ and $\langle I\rangle_{XYF} = \frac{1}{XYF}\sum_{x=1}^{X}\sum_{y=1}^{Y}\sum_{f=1}^{F} I(x,y,f)$ is the average intensity over all frames $F$. When inhomogeneities move slowly through the region of interest over the time scale of the experiment, the fast fluctuations in the whole image series can still be evaluated by performing a *moving average correction* (2):

$$I_{\mathrm{RICS}}(x,y,f) = I(x,y,f) - \langle I(x,y,f)\rangle_{\Delta F} + \langle I\rangle_{XYF}, \qquad \text{Eq. S3}$$

where $\langle I(x,y,f)\rangle_{\Delta F} = \frac{1}{2\Delta F+1}\sum_{f=-\Delta F}^{\Delta F} I(x,y,f)$ is the moving average series from frames ($f$-$\Delta F$) to frame ($f$+$\Delta F$) and $\langle I\rangle_{XYF}$ is the average pixel intensity of a region of $X$×$Y$ over all frames $F$ . This procedure removes slowly moving spatial inhomogeneities that might lead to an erroneous RICS calculation result. After this correction, the mean intensity of each image will be equal to the mean pixel intensity throughout the experiment.

***Image pre-processing for N&B***

For N&B analysis, the temporal pixel variance in a PIE-FI image should be determined by only the molecular diffusion and the shot noise of the experiment, which is distributed Poissonian (3). Assuming the intensity is homogeneously distributed in the image, slow

temporal variations in intensity due to sample photobleaching, drift or laser instability can be corrected using a *frame mean subtraction* followed by *addition of the mean pixel intensity over the entire experiment:*

$$I_{\mathrm{NB}}(x,y,f) = I(x,y,f) - \langle I(f)\rangle_{XY} + \langle I\rangle_{XYF}, \qquad \text{Eq. S4}$$

where $I(x,y,f)$ is the photon count of pixel $(x,y)$ in frame $f$, $\langle I(f)\rangle_{XY} = \frac{1}{XY}\sum_{x=1}^{X}\sum_{y=1}^{Y} I(x,y,f)$ is the average intensity of frame $f$ and $\langle I\rangle_{XYF} = \frac{1}{XYF}\sum_{x=1}^{X}\sum_{y=1}^{Y}\sum_{f=1}^{F} I(x,y,f)$ is the average intensity over all frames $F$. When $\langle I\rangle_{XYF}$ is added to all pixels, the mean frame intensity will be constant while both the spatial and temporal pixel variance remains similar to the original data. When the image intensity is not distributed homogeneously, a local correction can be performed using a *per-pixel moving average subtraction followed by the addition of the pixel mean* (4):

$$I_{\mathrm{NB}}(x,y,f) = I(x,y,f) - \langle I(x,y,f)\rangle_{\Delta F} + \langle I(x,y)\rangle_{F}, \qquad \text{Eq. S5}$$

where $\langle I(x,y,f)\rangle_{\Delta F} = \frac{1}{2\Delta F+1}\sum_{f=-\Delta F}^{\Delta F} I(x,y,f)$ is the moving average and $\langle I(x,y)\rangle_{F} = \frac{1}{F}\sum_{f=1}^{F} I(x,y,f)$ is the average intensity of pixel $(x,y)$ over the whole image series. This correction preserves the spatial variance, and the variance from fast temporal fluctuations due to diffusing molecules. As the number of photons detected per pixel in a PIE-FI image is very low, even a moving average about a single pixel has insufficient statistics to reliably correct the N&B data. To circumvent this difficulty, one can perform spatial averaging in addition to the temporal moving average when the PSF is oversampled, as is the case for our N&B experiments:

$$I_{NB}(x,y,f) = I(x,y,f) - \langle I(x,y,f)\rangle_{\Delta(XYF)} + \langle I(x,y)\rangle_{F}, \qquad \text{Eq. S6}$$

where $\langle I(x,y,f)\rangle_{\Delta(XYF)} = (2\Delta X+1)^{-1}(2\Delta Y+1)^{-1}(2\Delta F+1)^{-1}\sum_{f=-\Delta F}^{\Delta F}\sum_{y=-\Delta Y}^{\Delta Y}\sum_{x=-\Delta X}^{\Delta X} I(x,y,f)$ is the mean pixel intensity in the cuboid with sides $2\Delta X$+1, $2\Delta Y$+1 and $2\Delta F$+1 surrounding pixel ($x$,$y$,$f$). For the experiments presented here, values of $\Delta X$, $\Delta Y$ = 3 and $\Delta F$ = 10 were sufficient for a quantitative N&B analysis. After pre-processing the N&B data, the $n(x,y)$

and $\varepsilon(x,y)$ images can be further filtered using spatial averaging to increase the statistics per pixel and/or a median filter to remove outliers from the images.

***Absolute concentration determination***

With RICS and N&B, absolute concentrations can be determined. *In vitro*, the sample concentration is usually homogenously distributed and an uncorrelated fluorescent background can be assumed, the amplitude of the spatial ACFs/CCFs can be converted into concentrations without compromise. In cells, two conditions have to be fulfilled to quantitatively determine sample concentrations: (i) the absence of an immobile fraction has to be confirmed and (ii) any pre-analysis processing that is needed should not alter the temporal pixel variance encoded in the image by the diffusing molecules of interest. When, for example, a moving average correction is applied to RICS (Eq S 3), both these conditions are fulfilled when the spatial correlation image of this moving average does not exhibit significant correlation. Conversely, when the overall temporal variance of pixels is not significantly changed by any pre-analysis processing algorithm, one can assume that the concentration determined by the RICS analysis is correct.

## Determination of weighted lifetime filters

A lifetime-weighted analysis requires determination of the appropriate weighting filters for the different species. To calculate the filters, the microtime spectra of the pure species needs to be determined or estimated. One possibility is to measure the pure species independently. For example, when performing measurements at low concentration, the microtime histogram from a highly concentrated sample could be used as species 1 ($F_{\mathrm{GG},1}(t)$) and the corresponding microtime histogram from a measurement of pure water can be used for species 2 ($F_{\mathrm{GG},2}(t)$). Alternatively, when the pure species cannot be determined independently, an idealized microtime histogram can be generated. For example, if the decay is expected to be monoexponential with known decay time, the microtime spectra of this species *x* can be determined by convoluting the theoretical decay with the instrument response function:

$$F_{\mathrm{GG},x}(t) = F_{\mathrm{GG,IRF}}(t - t_{shift}) * \exp(-t/\tau_x) \quad \text{Eq. S7}$$

Once the pure microtime histograms are known, the filters are determined using:

$$\begin{matrix} filter1 \\ filter2 \end{matrix} = \left( \begin{vmatrix} F_{GG,1}(t) \\ F_{GG,2}(t) \end{vmatrix} \cdot [D] \cdot \begin{vmatrix} F_{GG,1}(t) \\ F_{GG,2}(t) \end{vmatrix}^{T} \right)^{-1} \cdot \begin{vmatrix} F_{GG,1}(t) \\ F_{GG,2}(t) \end{vmatrix} \cdot [D] \qquad \text{Eq. S8}$$

where [D] is the diagonal matrix constructed from the reciprocal values of the corresponding histogram $F_{GG}(t)$ of a low-signal sample. The lifetime weighting filters used for quantitative RICS measurements at low concentration are shown in Fig. 4 *C* and estimations of the filters for the FRETing and non-FRETing eGFP-mCherry tandems are plotted in Fig. 5 *E*.

# Supporting Table

**Table S1 – Expected performance of the FPs on our PIE-FI microscope.**

| | $\varepsilon_{\lambda max}$ [$M^{-1}$ $cm^{-1}$] | $\phi_F$ [%] | $\varepsilon_{475nm}$ [%] | $\varepsilon_{561nm}$ [%] | $T$ [%] | $\varepsilon_{R/G}$ [%] | β [%] | $R_0$ [Å] |
|---|---|---|---|---|---|---|---|---|
| eGFP | 55000 | 60 | 85 | ~0 | 61 | 2 | 5 | 51 |
| mVenus | 92200 | 57 | 24 | ~0 | 57 | 7 | 8 | 56 |
| mCherry | 72000 | 22 | 4 | 63 | 42 | n.d. | 100 | |

$\varepsilon_{\lambda max}$ is the extinction coefficient at the excitation maximum, $\phi_F$ is the fluorescence quantum yield, $\varepsilon_{475nm}$ and $\varepsilon_{561nm}$ are the percentage of maximum absorption at the laser wavelength, $T$ is the calculated percentage of transmission for the FP through the polychroic, dichroic and its normal emission filter, $\varepsilon_{R/G}$ is the calculated relative brightness of the FP in the red versus the green detection channel, $\beta$ is the calculated relative brightness of the FP versus mCherry FP in the red detection channel, *i.e.* the crosstalk (5), and $R_0$ is the calculated Förster radius when the FP is used with mCherry as a FRET acceptor. n.d. = not determined.

## Supporting Figures

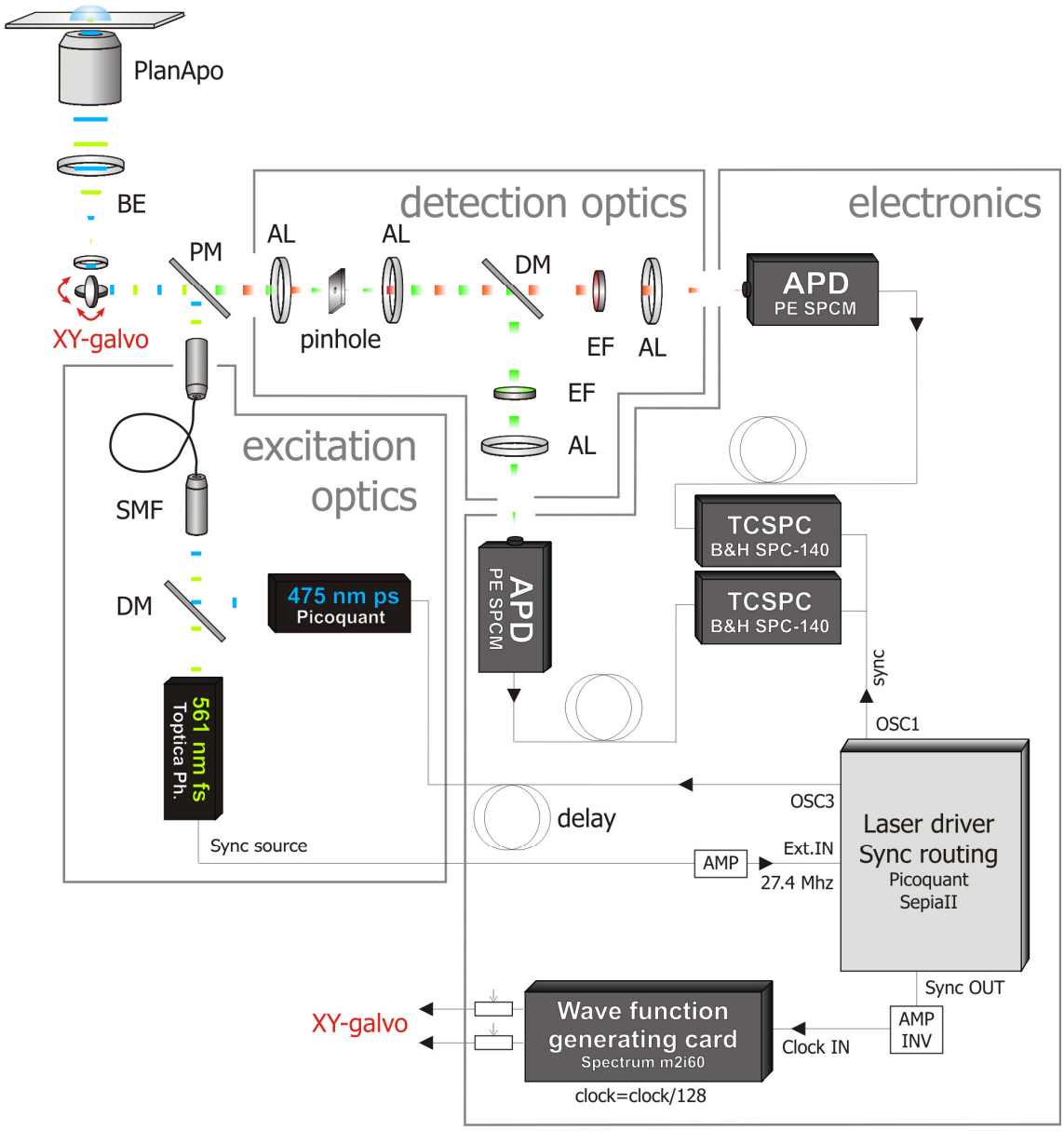


**Fig. S1 – Schematic illustration of the PIE-FI setup used in this work.** BE = beam expander, PM = polychroic mirror, AL = achromatic doublet lens, EF = emission filter, DM = dichroic mirror, SMF = single-mode fiber, OSC = oscillator module, AMP = signal amplifier, INV = signal inverter, galvo = galvanometric mirror scanner, APD = avalanche photodiode, sync = sychronization pulse.

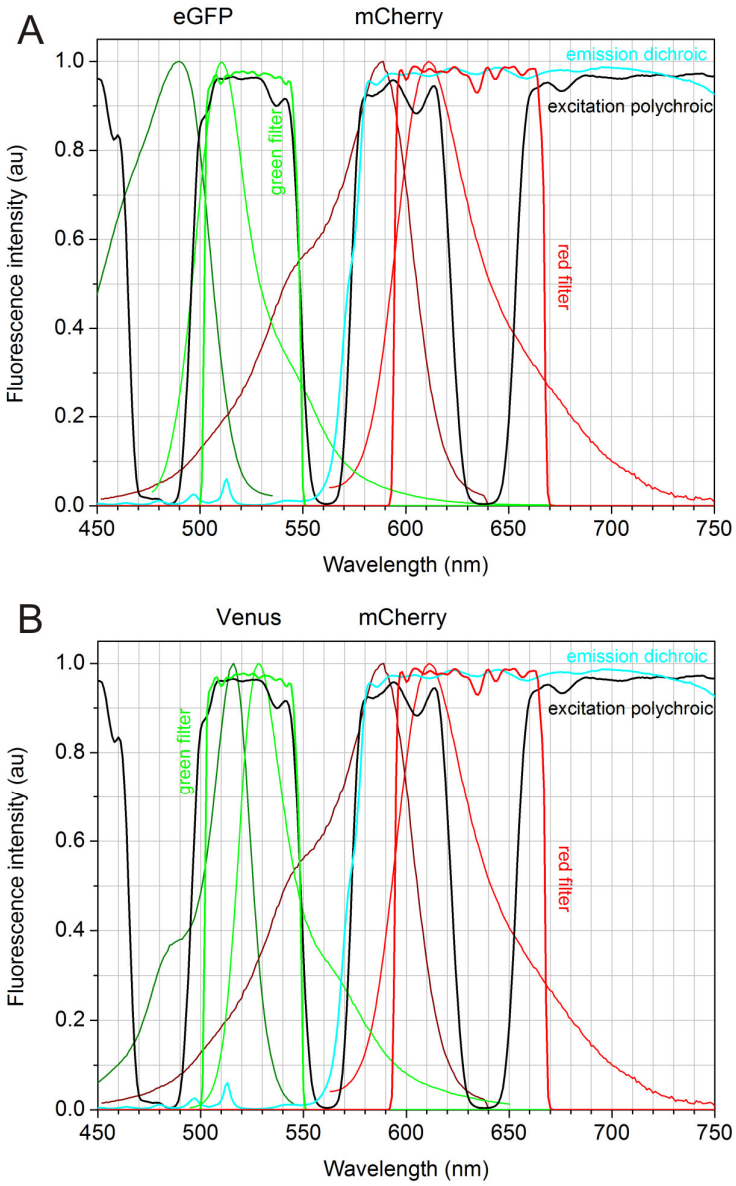


**Fig. S2 – Excitation and fluorescence spectra of the FPs used in this work.** The transmission spectra of the excitation polychroic, emission dichroic and emission filters, as described in the Supporting Materials and Methods section, were overlaid.

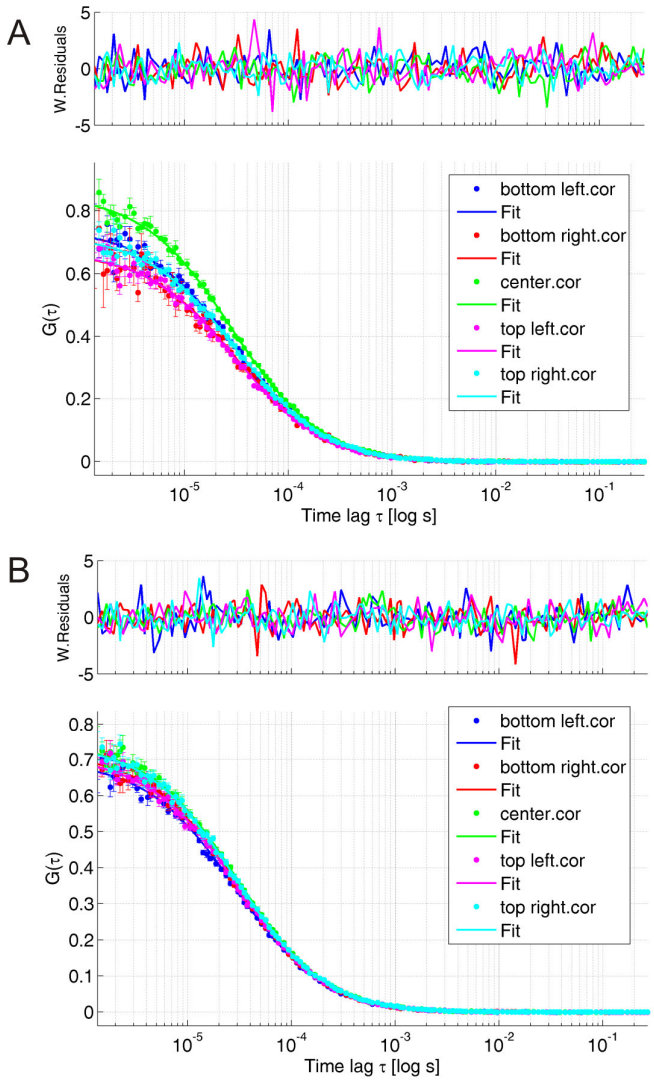


**Fig. S3 – Verification of the galvo and telescope alignment with point-FCS.** FCS ACFs of ATTO488 measured at the central or (0,0) position of the galvo scanner (drawn in *green*) or at the four respective corners (drawn in *blue, red, pink* and *cyan*) of a 100×100-µm² image (A) or 30×30-µm² image (B). The limited deviation in the corners confirmed a good alignment of the galvo and telescope in the excitation path. Importantly, all PIE-FI experiments were performed using a 12.5×12.5-µm² image range within the 100×100-µm² full range of the imaging system.

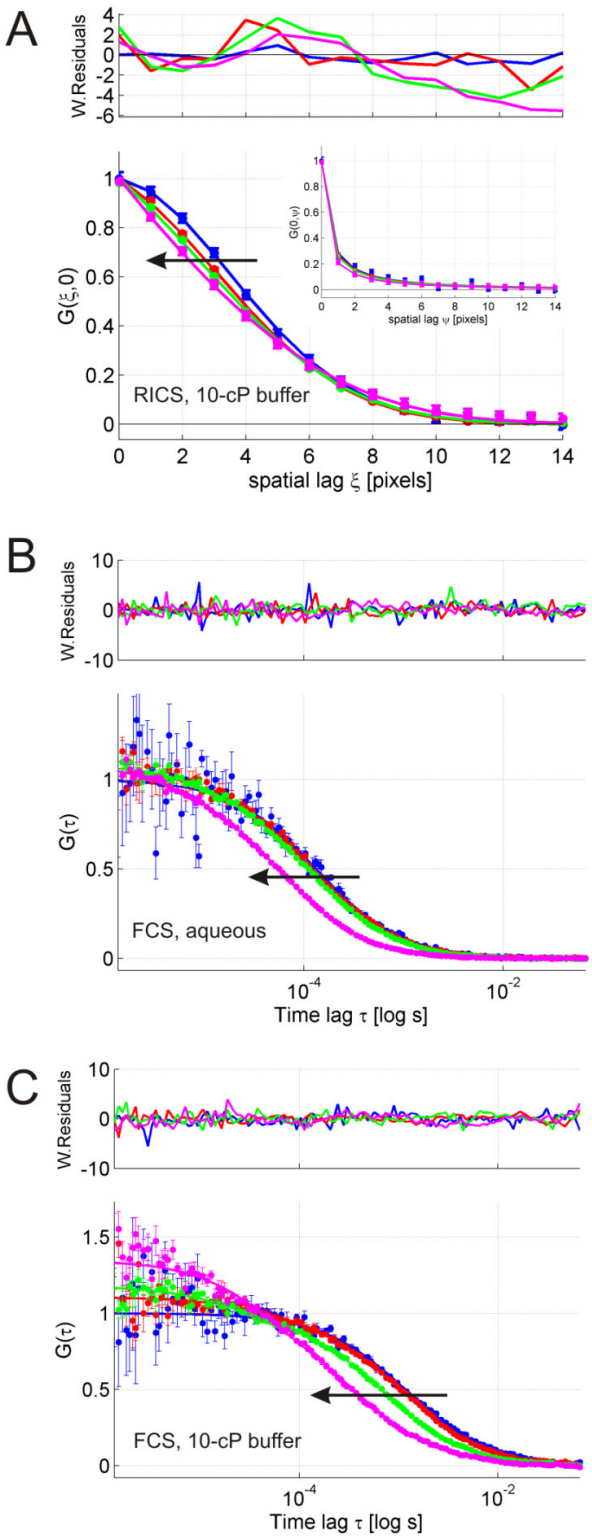


**Fig. S4 – Performance of RICS and FCS for measuring Venus as a function of laser power in an aqueous or 10-cP buffer.** (*A*) The experimental $G(\xi, 0)$ from PIE-RICS

(*symbols*) with fit (*line*) and weighted residuals is shown (*top graph*) for measurements at 2.5 µW (*blue*), 10 µW (*red*), 25 µW (*green*) and 100 µW (*pink*) excitation power. The $G(0,\psi)$ and fit are shown in the inset. The black arrow indicates the trend with increasing laser power. The correlation functions were normalized to the amplitude of the fit function by multiplying the data and fit with $N(1-F_{blink})/\gamma$. (*B* and *C*) The experimental $G(\tau)$ from PIE-FCS (*symbols*) with fit (*line*) and weighted residual are shown (*top graph*) for measurements at 2.5 µW (*blue*), 10 µW (*red*), 25 µW (*green*) and 100 µW (*pink*) excitation power in aqueous solution (A) and in a 10-cp sucrose/buffer mixture (B). The black arrow indicates the trend with increasing laser power. The correlation functions were normalized to the amplitude of the fit function by multiplying the data and fit with $N(1-F_{blink})/\gamma$.

## Supporting References

1. Digman, M. A., C. M. Brown, P. Sengupta, P. W. Wiseman, A. R. Horwitz, and E. Gratton. 2005. Measuring Fast Dynamics in Solutions and Cells with a Laser Scanning Microscope. Biophys J 89:1317-1327.
2. Brown, C. M., R. B. Dalal, B. Hebert, M. A. Digman, A. R. Horwitz, and E. Gratton. 2008. Raster image correlation spectroscopy (RICS) for measuring fast protein dynamics and concentrations with a commercial laser scanning confocal microscope. J.Microsc. 229:78-91.
3. Hillesheim, L. N. and J. D. Muller. 2005. The dual-color photon counting histogram with non-ideal photodetectors. Biophys J 89:3491-3507.
4. Digman, M. A., R. Dalal, A. F. Horwitz, and E. Gratton. 2008. Mapping the Number of Molecules and Brightness in the Laser Scanning Microscope. Biophys J 94:2320-2332.
5. Müller, B. K., E. Zaychikov, C. Bräuchle, and D. C. Lamb. 2005. Pulsed Interleaved Excitation. Biophys J 89:3508-3522.